Outer membrane vesicles can contribute to cellulose degradation in *Teredinibacter turnerae,* a cultivable intracellular endosymbiont of shipworms

Mark T. Gasser[a]# | Annie Liu[a] | Marvin Altamia[b] | Bryan R. Brensinger[a] | Sarah L. Brewer[a] | Ron Flatau[b] | Eric R. Hancock[a] | Sarah P. Preheim[c] | Claire Marie Filone[a] | Dan L. Distel[b]#

[a]Johns Hopkins University Applied Physics Laboratory, Laurel, Maryland, USA 20723

[b]Ocean Genome Legacy Center, Northeastern University, Nahant, Massachusetts, USA 01908

[c]Johns Hopkins University, Baltimore, Maryland, USA 21218

Running title: Cellulolytic Outer Membrane Vesicles from *T. turnerae*

Keywords: carbohydrate-active enzymes, CAZymes, lignocellulose degradation, OMVs, protein secretion, symbiosis, *tonB*-dependent receptors

MTG: mark.gasser@jhuapl.edu (ORCID: 0000-0002-9396-4954) #Co-corresponding author

AL: annie.liu@jhuapl.edu (ORCID: 0009-0002-3224-6008)

MAA: marvin.altamia@gmail.com (ORCID: 0000-0002-8625-767X)

BRB: bryan.brensinger@jhuapl.edu (ORCID: 0009-0002-0327-021X)

SLB: sarah.brewer@jhuapl.edu (ORCID: 0009-0007-9039-0784)

RF: r.flatau@northeastern.edu (ORCID: 0000-0002-4357-5870)

ERH: eric.hancock@jhuapl.edu (ORCID: 0009-0002-3041-2148)

SPP: sprehei1@jhu.edu (ORCID: 0000-0001-7365-2382)

CMF: claire.marie.filone@jhuapl.edu (ORCID: 0000-0002-4041-3948)

DLD: d.distel@northeastern.edu (ORCID: 0000-0002-3860-194X) #Co-corresponding author

Data availability

The authors confirm that the data supporting this study's findings are available within the article and its supplementary materials. The mass spectrometric raw files are accessible at https://massive.ucsd.edu under accession MassIVE MSV000094250 and at https://www.proteomexchange.org under accession PXD050419.

Funding statement

Research reported in this publication was supported by the following awards to DLD: National Oceanic and Atmospheric Administration (NA19OAR0110303), Gordon and Betty Moore Foundation (GBMF 9339), National Institutes of Health (1R01AI162943-01A1, subaward: 10062083-NE), and JHU/APL Internal Research and Development. The National Science Foundation (DBI 1722553) also funded some equipment used in this research.

Conflict of interest statement

The authors report no conflict of interest. The funders had no role in study design, data collection, interpretation, or the decision to submit the work for publication.

Abstract

Teredinibacter turnerae is a cultivable cellulolytic Gammaproeteobacterium (Cellvibrionaceae) that commonly occurs as an intracellular endosymbiont in the gills of wood-eating bivalves of the family Teredinidae (shipworms). The genome of *T. turnerae* encodes a broad range of enzymes that deconstruct cellulose, hemicellulose, and pectin and contribute to lignocellulose digestion in the shipworm gut. However, the mechanism by which symbiont-made enzymes are secreted by *T. turnerae* and subsequently transported to the site of lignocellulose digestion in the shipworm gut is incompletely understood. Here, we show that *T. turnerae* cultures grown on carboxymethyl cellulose (CMC) produce outer membrane vesicles (OMVs) that contain a variety of proteins identified by LC-MS/MS as carbohydrate-active enzymes with predicted activities against cellulose, hemicellulose, and pectin. Reducing sugar assays and zymography confirm that these OMVs retain cellulolytic activity, as evidenced by hydrolysis of CMC. Additionally, these OMVs were enriched with *TonB*-dependent receptors, which are essential to carbohydrate and iron acquisition by free-living bacteria. These observations suggest potential roles for OMVs in lignocellulose utilization by *T. turnerae* in the free-living state, in enzyme transport and host interaction during symbiotic association, and in commercial applications such as lignocellulosic biomass conversion.

Introduction

The biological degradation of lignocellulose, a primary component of wood and all plant biomass, is a critical process in the global carbon cycle and has potential applications in renewable energy and chemical production through biomass conversion (Ragauskas *et al.*, 2014; Østby *et al.*, 2020). Lignocellulose is a complex composite material composed primarily of microfibrils of cellulose, the most abundant organic polymer on Earth (Dahmen *et al.*, 2019), embedded in a matrix of hemicellulose and lignin. Pectins may also be present in smaller quantities. However, due to its complexity, lignocellulose degradation requires a suite of specialized enzymes to convert its component polymers into accessible nutrients. This complexity precludes most organisms from utilizing lignocellulose and creates obstacles to bioconversion to renewable fuels or fine chemicals (Cragg *et al.*, 2015).

One of the unique biological systems where efficient wood digestion occurs is found within shipworms, a group of marine bivalve mollusks of the family Teredinidae and the primary degraders of woody plant material in mangrove forests and in association with driftwood and marine woodfalls (Voight, 2015; Cragg *et al.*, 2020). Shipworms harbor endosymbiotic bacteria in bacteriocytes confined to the gland of Deshayes, a tissue located within their gills (Distel *et al.*, 1991). The genomes of these bacteria, primarily from the genus *Teredinibacter*, encode a wide variety of enzymes targeting lignocellulose (Distel *et al.*, 2002; Yang *et al.*, 2009; O'Connor *et al.*, 2014; Altamia, Shipway, *et al.*, 2020; Altamia *et al.*, 2021) and express them within this gland (O'Connor *et al.*, 2014; Sabbadin *et al.*, 2018). The resulting bacterial enzymes are also found in the shipworm's cecum (O'Connor *et al.*, 2014; Sabbadin *et al.*, 2018; Altamia and Distel, 2022), a specialized organ that is the primary location of wood digestion for the shipworm and is nearly devoid of microbes (Betcher *et al.*, 2012). This physical separation

between the bacterial symbionts in the gill and wood digestion in the gut requires a transport mechanism for symbiont-made cellulolytic enzymes. Recently, a system of ducts called the ducts of Deshayes was shown to serve as an extracellular transport path for bacterial cellulases from the gills to the mouth of shipworms (Altamia and Distel, 2022). However, the mechanism by which enzymes produced by the intracellular bacteria move across multiple membranes to an external transport path is still unknown.

Bacteria use a variety of mechanisms to degrade lignocellulosic substrates in their environments. For example, polysaccharide-degrading bacteria, including the common rumen bacteria *Bacteroides*, *Clostridia*, and *Fibrobacter,* use the type IX secretion pathway (T9SS) to secrete large molecular-weight proteins, including multidomain carbohydrate-active enzymes (CAZymes) (Gharechahi *et al.*, 2023). These enzymes may be released into the environment or bound to the cell envelope (McGavin *et al.*, 1990; Cai *et al.*, 1999; Yan and Wu, 2013). In addition to the secretion of soluble or membrane-bound enzymes, bacteria may export CAZymes by producing outer membrane vesicles (OMVs). OMVs are spherical buds that originate from the bacterial outer membrane and can contain various cellular components such as lipopolysaccharides, proteins, small molecules, and nucleic acids (Schwechheimer and Kuehn, 2015; Huang *et al.*, 2022).

Recent studies have shown that OMVs can be highly enriched in CAZymes and retain activity capable of degrading cellulose and other plant biomass (Arntzen *et al.*, 2017; Ichikawa *et al.*, 2019; Salvachúa *et al.*, 2020). The majority of research on OMVs has been done on pathogenic bacteria due to the capacity of OMVs to carry and deliver virulence factors and toxins into host cells (O'Donoghue and Krachler, 2016; Lynch and Alegado, 2017; Caruana and

Walper, 2020). However, the role of OMVs in marine and other environments has been increasingly recognized, likely playing crucial roles in nutrient processing and ecological interactions (Frias *et al.*, 2010; Biller *et al.*, 2014, 2022; Fischer *et al.*, 2019; Fadeev *et al.*, 2023). *Teredinibacter turnerae*, unlike obligate intracellular symbionts, is also capable of free-living growth (Waterbury *et al.*, 1983) and may directly acquire carbon from cellulose or other plant biomass in the marine environment (Naka and Haygood, 2023). Investigating the functionality of OMVs in *T. turnerae* could be pivotal to understanding their complex symbiotic interaction and the ecological impact of their dual lifestyle.

Here, we purify and characterize the protein composition of OMVs produced by *T. turnerae* during growth on water-soluble carboxymethyl cellulose (CMC). Proteins putatively involved in interactions with lignocellulose were identified by LC-MS/MS analysis and comparison to the Carbohydrate Active Enzyme Database (CAZy). Additionally, activity assays were used to show that OMVs produced by *T. turnerae* are capable of cellulose hydrolysis. These observations suggest that OMVs contribute to cellulose utilization by *T. turnerae* and may play essential roles in their metabolism in free-living and symbiotic states.

Experimental Procedures

Strain isolation, selection, and growth conditions

T. turnerae is an endosymbiont species with widespread occurrence among shipworm species (Distel *et al.*, 2002; Altamia *et al.*, 2014; Altamia, Lin, *et al.*, 2020). Two strains were selected: *T. turnerae* T7901 (ATCC 39867), which was previously isolated from *Bankia gouldi* and was the first shipworm symbiont brought into pure culture (Waterbury *et al.*, 1983; Distel *et al.*, 2002; Yang *et al.*, 2009); and *T. turnerae* SR01903, a closely related strain of *T. turnerae* (Altamia *et al.*, 2014). *T. turnerae* SR01903 was isolated from the gills of a single specimen of *Lyrodus*

pedicellatus found in naturally occurring driftwood collected by hand in shallow water in the Indian River Lagoon, Merit Island, FL. (N 28.40605 W 80.66034) on January 24, 2020. Gills were removed by dissection and homogenized in 1.0 ml of SBM medium (Waterbury *et al.*, 1983) in an autoclave-sterilized glass dounce homogenizer. Homogenate was streaked onto a culture plate containing 1.0% Bacto agar shipworm basal medium (SBM) at pH 8.0 supplemented with 0.2% w/v powdered cellulose (Sigmacell Type 101; Sigma-Aldrich) and 0.025% NH_4Cl. Plates were incubated at 30 °C until individual colonies could be observed. An individual colony was then picked and subjected to multiple rounds of restreaking from single colonies to ensure clonality. To identify the isolate, the 16S rRNA gene was PCR amplified, sequenced, and compared to published *T. turnerae* genomes. The complete genome of *T. turnerae* SR01903 was then sequenced (SRA number SRR28421271) and submitted to Genbank (Submission number SUB14332655, Bioproject PRJNA1090931, assembly accession number pending; assembly and annotation files provided in additional files for review but not for publication). For the experiments described herein, strains were initially propagated in 6 mL cultures in shipworm basal medium (Waterbury *et al.*, 1983) supplemented with 0.025% NH_4Cl and 0.2% carboxymethyl cellulose for 4 days before being diluted 1/250 in fresh media and harvested after 2 days (OD600 0.2-0.3). All cultures were incubated in a shaker incubator at 30 °C and 100 rpm. An overview of the procedures conducted in this research is presented in Figure 1.

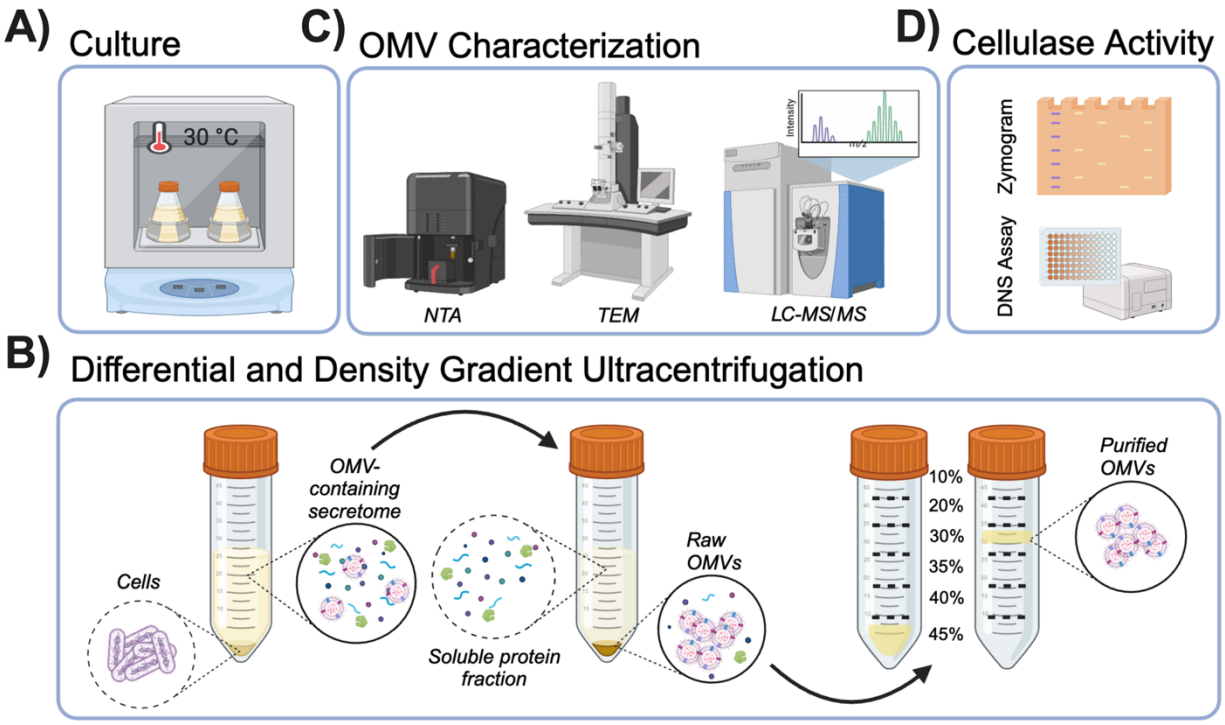

Figure 1. Methods used to isolate and characterize outer membrane vesicles from T. turnerae. Diagram showing: (A) bacterial culture, (B) OMV isolation based on differential and density gradient separation, (C) OMV visualization and size by TEM and NTA, proteome analysis by LC-MS/MS, and (D) detection of cellulase activity in purified OMV preparations by zymography and reducing sugar (DNS) assay. Created with BioRender.com

Isolation of Outer Membrane Vesicles (OMVs)

Bacterial cells were separated from the culture supernatant by centrifugation at 5,000 x g for 20 minutes at 4 °C. The supernatant was then transferred to a fresh tube, and centrifugation was repeated to remove residual bacterial cells. The final supernatant was carefully collected without disturbing the remaining pellet and filtered through a 0.22 µm polyethersulfone filter as an additional precaution to remove cells. The putative OMVs were then pelleted from the filtrate by ultracentrifugation at 120,000 x g (T-647.5 rotor, Sorvall) for 90 minutes at 4 °C. For purification, the resulting pellet was resuspended in 0.1 M phosphate-buffered saline (PBS) and fractionated by bottom-up density gradient ultracentrifugation using Optiprep™ (iodixanol density gradient medium) as follows. The resuspended OMV-containing pellet was mixed with 60% iodixanol solution to a final density of 45% (w/v) and placed at the

bottom of an ultracentrifuge tube. A discontinuous density gradient was generated using a syringe and G21 needle to deposit layers of 40%, 35%, 30%, 20%, and 10% iodixanol with a final layer of 0.25 mL 0.1 M PBS on top. The resulting gradient was then subjected to centrifugation for 16 hours at 150,000 x g and 4 °C (SW55 Ti rotor, Beckman-Coulter). Sample banding was visually observed at the interface of the 30% and 20% fractions (Supporting Information: Figure S1). All fractions were collected, and iodixanol was removed by passive diffusion dialysis (1,000 kDa MWCO) in exchanging buffer of 50 mM ammonium bicarbonate pH 8.3 at 4 °C. OMV samples were removed from the dialysis bag and concentrated under vacuum to 100 µL (SPD121P SpeedVac, Thermo Scientific). Particle visualization and characterization proceeded with the single 30% fraction.

Transmission electron microscopy (TEM)

Purified OMVs were diluted and absorbed onto 200 mesh formvar-treated and carbon-coated copper grids for 60 seconds. Samples were then fixed for 5 minutes in 4% glutaraldehyde in 0.1 M sodium cacodylate, and grids were stained with 1% aqueous uranyl acetate for 60 seconds and left to dry. OMVs were imaged in an FEI Tecnai T12 (Thermo Fisher) transmission electron microscope at 80 KV with an AMT bottom-mount camera.

Nanoparticle tracking analysis (NTA)

NTA was performed using the ZetaView® PMX-220 Twin (Particle Metrix) configured with 488 nm and 640 nm lasers with long wave-pass cut-off filters (500 nm and 660 nm, respectively) and a sensitive CMOS camera 640 x 480 pixels. Samples were diluted in 2 mL of 0.1 µm filtered deionized water (18 MΩ/cm) to obtain a particle concentration between 1 x 10^7 and 1 x 10^8 particles/mL. The instrument was set to a sensitivity of 80, a shutter speed of 100, and a frame rate of 30 frames per second. Each sample was measured at 11 different positions throughout

the sample cell, with 1 cycle of reading at each position to have a minimum of 1,000 traces. If the number of traces was below 1,000 counts, some additional sample was flushed inside the sample cell, and the acquisition was repeated. Post-acquisition parameters were set to a minimum brightness of 20, a maximum size area of 1,000 pixels, a minimum size area of 10 pixels, and tracelength of 15 frames. Automated cell quality control was checked using high-quality deionized water. Camera alignment and focus optimization were performed using polystyrene Nanosphere™ 100 nm size standard beads. Data analysis was performed with ZetaView® 8.05.14 software provided by the manufacturer. Automated reports of the particle recordings across the 11 positions were manually checked, and any outlier position was removed to calculate particle concentration and distribution.

Proteomic analysis

OMVs were lysed and denatured in a solution containing 5% sodium dodecyl sulfate (SDS), 100 mM Tris (pH=8), 20 mM chloroacetamide, and 10 mM tris (2-carboxyethyl) phosphine hydrochloride and incubated at 90 °C for 10 minutes. Proteins were aggregated and isolated using Sera-Mag™ carboxylate-modified SpeedBeads (SP3 beads) and digested in 100 mM NH_4HCO_3 containing Trypsin (final concentration 6 ng/µL) overnight at 37 °C and 1,200 rpm. Digested samples were loaded onto C18 tips, and peptides were separated online using an 88-minute LC gradient (Evosep LC system). MS analysis was performed on a Q-Exactive HF-X Hybrid Orbitrap mass spectrometer (Thermo Scientific). One full high-resolution MS spectrum was acquired with a resolution of 45,000, an AGC target of 3×10^6 with a maximum ion time of 45 ms, and a scan range of 400-1,500 m/z, followed by 20 HCD MS/MS scans with a resolution of 1,5000, an AGC target of 1×10^5 with a maximum ion time of 120 ms, NCE of 27, and isolation window of 2 m/z. The resulting MS/MS spectra were searched against the strain-specific and

209 universal contaminant protein databases using Sequest within Proteome Discoverer 1.4.
210 Identifications were filtered to include only high-confidence peptides based on a better than 1%
211 false discovery rate (FDR) against a decoy database. Proteins were linked to peptides, and only
212 proteins with >2 peptide spectral matches (PSM) with two unique peptides were kept
213 (Supporting Information: Dataset S1).

214 ## Functional characterization of OMV proteins

215 Identified proteins were annotated against the Clusters of Orthologous Groups (COG) of
216 proteins database (Galperin *et al.*, 2021), and their subcellular locations were predicted using
217 CELLO v2.5 (http://cello.life.nctu.edu.tw/) (Yu *et al.*, 2006) and PSORTdb v4.0
218 (https://db.psort.org/) (Lau *et al.*, 2021). Enrichment and functional associations between
219 proteins were determined by STRINGdb v11 (https://string-db.org/) (Szklarczyk *et al.*, 2019) and
220 ShinyGO v0.8 (http://bioinformatics.sdstate.edu/go/) (Ge *et al.*, 2020). Settings were selected to
221 use all coding sequences in the T7901 genome as background and a minimum FDR stringency of
222 1×10^{-5}. We then established which OMV proteins are predicted to exhibit carbohydrate-active
223 properties using the annotated T7901 genome in the Carbohydrate Active Enzymes Database
224 (CAZy, https://cazy.org).

225 ## Enzymatic activity assays

226 The cellulolytic activity of proteins in OMV preparations was visualized and size
227 fractionated by denaturing polyacrylamide gel electrophoresis (SDS-PAGE, 1.5 mm thickness, 9%
228 acrylamide, and 0.2% CMC final concentration). For zymographic analysis, 14 µg of protein
229 sample determined by Pierce 660 assay (Thermo Scientific) using bovine serum albumin as
230 standard were heat denatured by boiling for 3 minutes in SDS without a reducing agent to
231 facilitate recovery of activity after refolding and added to each lane. After electrophoresis, the

SDS-PAGE gel was transferred to 500 mL of refolding buffer (20% isopropanol, 0.1% Triton X-100 in 1x PBS, pH 7.4) and gently shaken for 1 hour at room temperature. The gel was then incubated in fresh 1x PBS buffer, pH 7.4, for 16 hours at room temperature before being stained with 0.1% Congo Red in 1x PBS buffer, pH 7.4 for 1 hour. The zymogram was destained with 1 M NaCl overnight to visualize regions where cellulase activity removed CMC. Additionally, the production of reducing ends was measured by the colorimetric 3,5-dinitrosalicylic acid (DNS) method (Ghose, 1987). Reactions were carried out in 96-well plates containing 50 µL 1% CMC, 30 µL 50 mM citrate buffer, and 20 µL purified OMV suspension and incubated for 4 hours at 37 °C. Next, 900 µL of DNS was added to each reaction, and reactions were heated at 99 °C for 10 minutes. Absorbance was measured at 540 nm, and sugar concentration was calculated by comparison to a glucose standard curve. The enzyme activity unit was defined as the amount of enzyme that liberated 1 µmol of reducing sugar per minute.

Results

OMV isolation and characterization

OMVs were isolated from cell-free supernatants of two closely related strains, T7901 and SR01903, by density gradient ultracentrifugation. The presence of OMVs was confirmed by NTA and TEM (Figure 2 A-D). The mean concentration of particles and average particle diameter size determined by NTA were 1.67 x 10^9 particles/mL and 162.5 $\pm$ 49.7 nm for T7901 and 1.30 x 10^9 particles/mL and 206.6 $\pm$ 61.7 nm for SR01903. TEM images (Figure 2 C-D) show that the putative OMV-enriched fractions from strains T7901 and SR01903 contain particles with size distribution and morphology typical of bacterial OMVs.

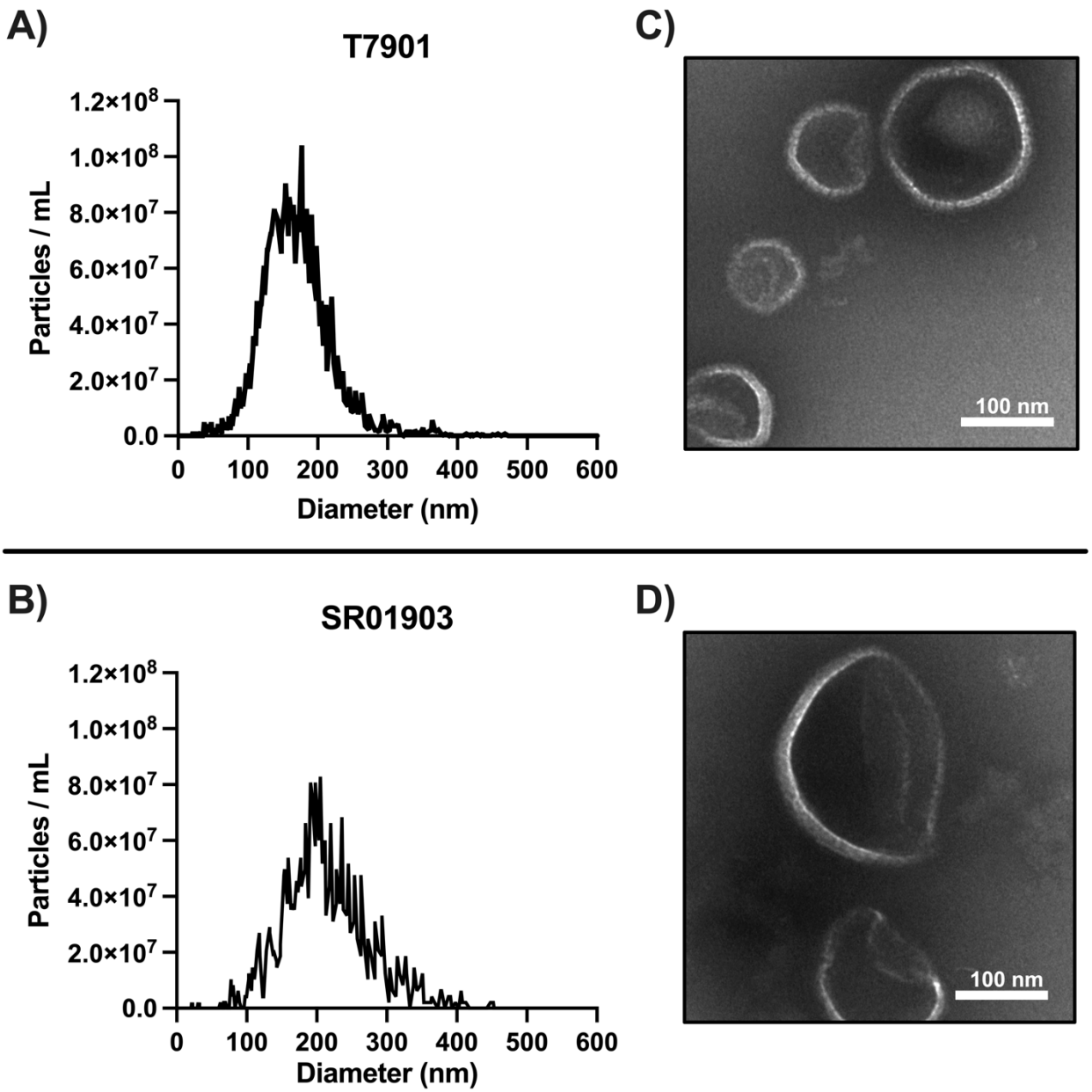

Figure 2. Size, concentration, and visualization of OMVs isolated from T. turnerae culture supernatants after growth on carboxymethyl cellulose (CMC). (A-B) Size distribution and particle concentration for strains T7901 and SR01903, respectively. OMVs from SR01903 were slightly larger in average size than OMVs from T7901. *(C-D) Isolated OMVs from strains T7901 and SR01903 were imaged using transmission electron microscopy. Scale bar = 100 nm.*

OMV proteome analysis

The protein contents of OMVs from both strains were analyzed by LC-MS/MS. Peptide-generated data were used to search against T7901 and SR01903 annotated protein sequences to identify OMV proteins and their relative abundance. A cut-off of two or more unique

predicted peptides per identified protein was used, resulting in the identification of 472 and 569 proteins for T7901 and SR01903, respectively. The Top 100 most abundant proteins identified in T7901 and SR01903 represented 81% and 74% of the total peptide content, respectively. Among those proteins, 71 were identified in both strains, indicating that the two strains produce a common core set of OMV proteins when grown under the examined culture condition. After protein identification, PSORTdb v4.0 (Lau *et al.*, 2021) and CELLO v2.5 (Yu *et al.*, 2006) were used to predict the subcellular location of all identified proteins. Outer membrane proteins comprised most (~75% and ~60%, respectively) of the OMV protein content of both T7901 and SR01903 (Figure 3 A). OMV proteins were clustered into orthologous groups (COG); 65% and 60% of OMV proteins for T7901 and SR01903 were assigned a single cluster, respectively. Most OMV proteins assigned to clusters in both strains were categorized as Cell Wall/Membrane/Envelope Biogenesis, Inorganic Ion Transport and Metabolism, and Carbohydrate Transport and Metabolism (Figure 3 B).

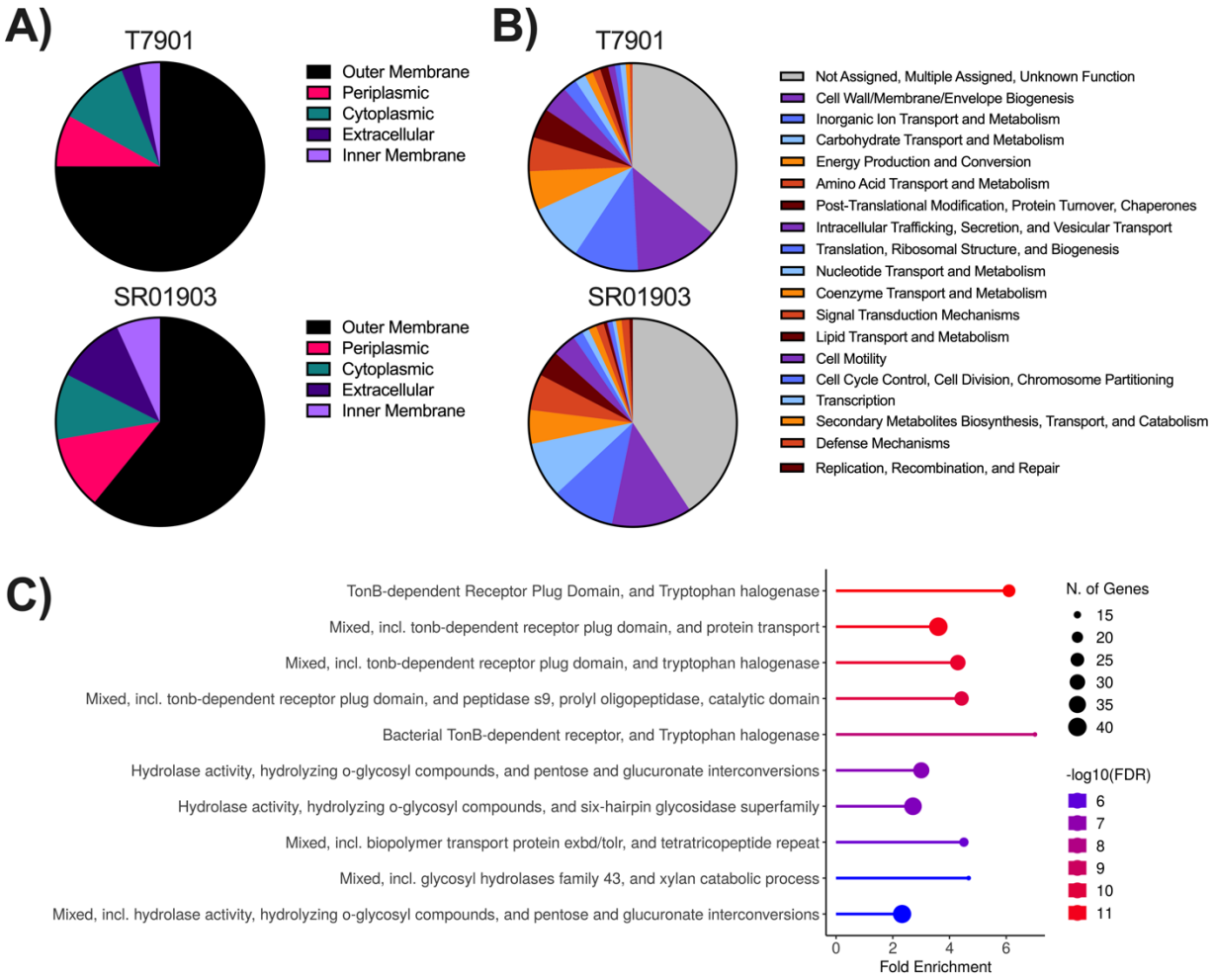

Figure 3. T. turnerae OMV proteome profiles. (A) Relative protein abundance grouped by predicted subcellular location and (B) Clusters of Orthologous Groups (COG) functional categories of identified proteins. (C) Top 10 STRINGdb pathways (ranked by FDR) found in OMVs of T7901. Similar top pathways were found in OMVs of SR01903.

TonB-dependent receptors and glycosyl hydrolase activity are enriched in OMVs

To highlight functional associations, OMV protein content was analyzed using STRING (Szklarczyk *et al.*, 2019) enrichment. We found significant enrichment of pathways involving *TonB*-dependent receptors (TBDR) and glycosyl hydrolase activity (Figure 4 C). The most abundant proteins were TBDRs, which constituted ~47% and ~44% of the OMV protein content in T7901 and SR01903, respectively. TBDRs are known to be deployed for the uptake of sugars from complex carbohydrates (Blanvillain *et al.*, 2007; Pollet *et al.*, 2021). Additionally, *TonB* knockouts of *T. turnerae* were shown to have lost the ability to grow on cellulose (Naka and

Haygood, 2023), which suggests that the *TonB* system in *T. turnerae* is critical to cellulose utilization.

Efficient utilization of lignocellulose for growth often requires a cocktail of multiple enzymes targeting inner (endo-acting) and outer (exo-acting) polysaccharide glycosidic bonds and various bonds found in heteroxylans. In total, 39 and 48 predicted CAZymes were present, representing 30 and 29 different catalytic CAZy families and 8.3% and 8.4% of identified OMV proteins in T7901 and SR01903, respectively. Most identified CAZy modules belong to glycoside hydrolase families (GH) predicted to be involved in cellulose and hemicellulose degradation (Figure 4 A) and that include several hydrolytic activities: endo-glucanases (GH5, GH8, GH9, GH10, GH11, GH26, GH44, GH45, GH51, GH62), exo-glucanases (GH5, GH9, GH26GH43GH26, GH43), and beta-glucosidases (GH2, GH3, GH5, GH39). In addition, multiple enzymes were predicted to include non-catalytic carbohydrate-binding modules (CBMs), which can enhance enzyme activity by increasing accessibility to the substrate (Hervé *et al.*, 2010).

Cellulase activity

Many OMV proteins were predicted to have or be associated with cellulolytic activity. We confirmed these by testing OMV suspensions for hydrolytic activity against CMC by zymography and reducing sugar DNS assay. In zymograms, clear zones indicating endoglucanase activity (Teather and Wood, 1982) were visualized between 95-130 kDa for both strains after 16-hour incubation (Figure 4 B). The production of reducing sugars from CMC was measured using DNS assay, and when normalized to total protein content, OMVs produced from SR01903 had the equivalent cellulolytic activity as a commercial soluble cellulase enzyme cocktail. Notably, OMVs produced from T7901 showed ~10x the activity of the commercial cellulase cocktail (Figure 4 C).

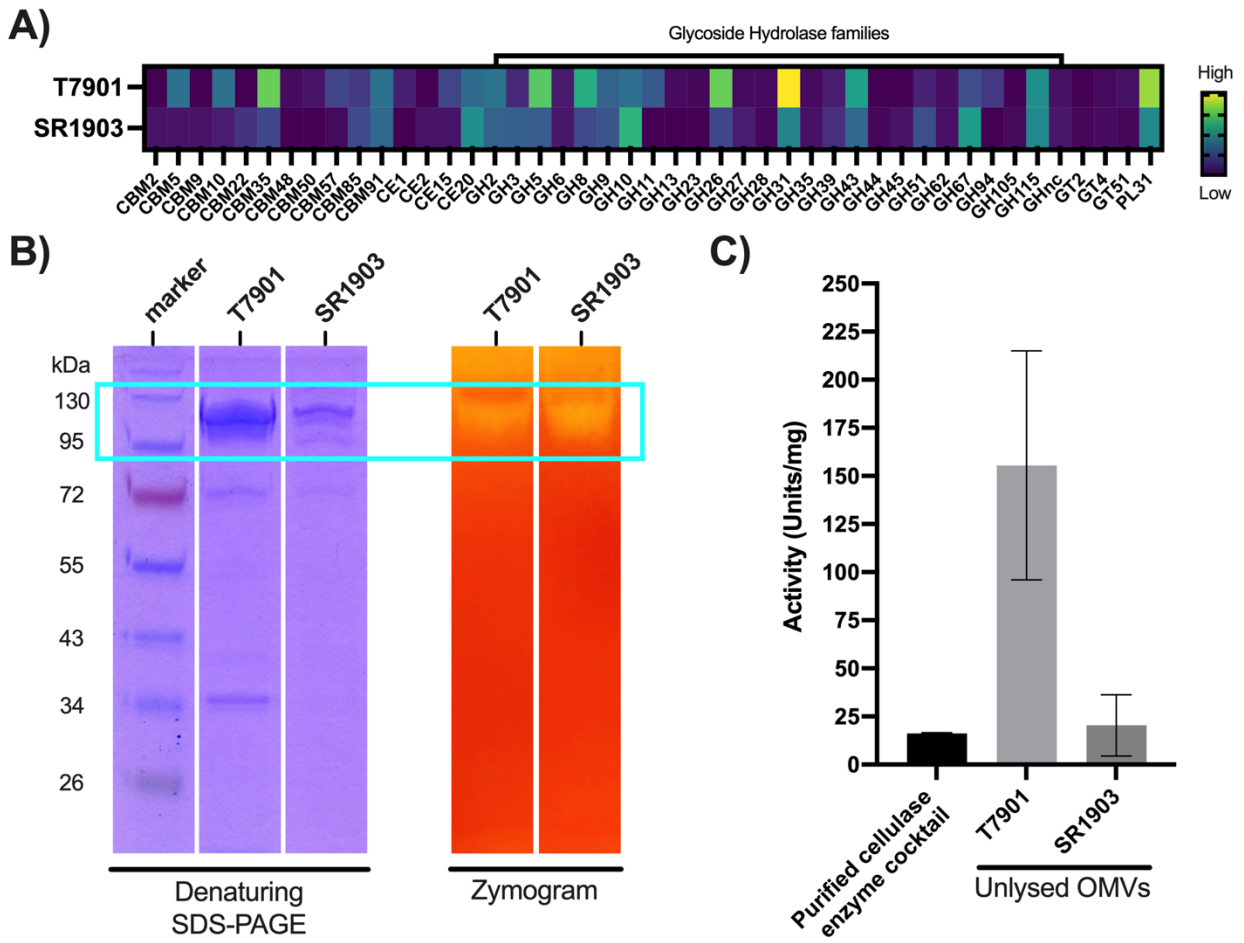

Figure 4. Carbohydrate-active modules and observed cellulase activity of T. turnerae OMVs. (A) Heatmap profile of the relative abundance of the predicted carbohydrate-active enzymes found in OMVs. (B) Denaturing SDS-PAGE (left) and zymogram (right; CMC substrate) of isolated OMVs. (C) Histogram showing cellulase activity (CMC substrate) in Units/mg (as determined by DNS assay) for isolated OMVs and a purified cellulase enzyme cocktail (Cellulase R-10, Goldbio CAS# 9012-54-8). Bars indicate means (error bars: standard deviations of three replicates).

Discussion

T. turnerae secretes a broad array of carbohydrate-active enzymes within the host's gills and when grown in pure culture (Yang *et al.*, 2009; O'Connor *et al.*, 2014; Sabbadin *et al.*, 2018). Genome sequence suggests these enzymes may be translocated across the inner membrane by Sec and Sec-independent (twin-arginine, Tat) pathways and through the outer membrane by the Type II (T2SS) generalized secretory pathway. The *T. turnerae* genome also encodes the complete Type VI secretion system (T6SS), which mediates many types of bacteria-bacteria and

bacteria-host interactions (Yang *et al.*, 2009). However, the role of OMVs in the transport of cellulolytic enzymes by *T. turnerae* has not been investigated. Here, we show that *T. turnerae* strains T7901 and SR01903 produce OMVs that contain diverse carbohydrate-active enzymes, including glycoside hydrolases, carbohydrate esterases, and polysaccharide lyase with predicted activity against cellulose, hemicellulose, and pectin. We further show that these OMV preparations can hydrolyze carboxymethyl cellulose (CMC) with specific activities comparable to or greater than that observed for a commercial purified cellulase enzyme cocktail (Figure 4 C).

In purified OMVs isolated from *T. turnerae* strains T7901 and SR01903, we detected representatives of 11 carbohydrate-binding module (CBM) families (CBM2, 5, 9, 10, 22, 35, 48, 50, 57, 85, and 91). Each of these families is known to bind cellulose or hemicellulose components, except for CBM50, which typically binds peptidoglycan or chitin. Additionally, catalytic modules representing 23 glycoside hydrolase (GH) families, four carbohydrate esterase (CE) families, and one polysaccharide lyase (PL) were detected. All of these GH families (GH2, 3, 5, 8, 9, 10, 11, 13, 23, 26, 28, 31, 35, 39, 43, 44, 45, 51, 62, 67, 94, 105, and 115) target bonds found within cellulose, hemicellulose or pectin, except GH23, which primarily acts on peptidoglycan. Finally, the four carbohydrate esterase (CE) families detected (CE1, 2, 15, and 20) target bonds found in hemicellulose, or bonds covalently linking hemicellulose to lignin. This combination of modules indicates a complete lignocellulose deconstruction system, including potential endo- and exo-activities against cellulose and hemicellulose backbones, debranching of hemicellulose sidechains, and hydrolysis of the resulting oligomers and monomers.

The fact that this wide array of activities was found in OMVs produced by cells of *T. turnerae* strains T7901 and SR01903 grown with cellulose as a sole carbon source indicates that

the expression of genes active against other lignocellulose components was either constitutive or co-regulated with expression of genes targeting cellulose. The ability of *T. turnerae* to express these activities in the absence of induction by their specific target substrates is consistent with the observation that shipworm endosymbionts express a wide range of lignocellulolytic enzymes when growing within the gill bacteriocytes of the host where they have no direct contact with lignocellulose (O'Connor *et al.*, 2014; Sabbadin *et al.*, 2018). Notably, six of the catalytic module families detected in *T. turnerae* OMVs (CE11, 15, and GH9, 10, 11, and 45) were also detected in the cecum content of *Bankia setacea* in a previous investigation (O'Connor *et al.*, 2014); however, it should be noted that this shipworm species hosts four *Teredinibacter* species, *T. waterburyi* (Altamia, Shipway, *et al.*, 2020), *T. franksiae*, *T. haidensis*, and *T. purpureus* (Altamia *et al.*, 2021) but does not harbor *T. turnerae* (O'Connor *et al.*, 2014).

While diverse CAZymes are present in the OMV proteome of *T. turnerae*, they comprise less than 10% of the total protein content of OMVs produced under the conditions examined here. Interestingly, the most abundant proteins observed were identified as TonB-dependent receptors (TBDR), accounting for nearly half of the proteins detected. TBDR enrichment has been previously reported in OMVs of several Gram-negative bacteria (Veith *et al.*, 2015; Zakharzhevskaya *et al.*, 2017; Dhurve *et al.*, 2022; Fadeev *et al.*, 2023). TBDRs are outer membrane-associated proteins that bind and mediate the energy-dependent movement of siderophores and various nutrients, including carbohydrates that are too large to be taken up via transmembrane diffusion across the outer membrane (Silale and Van Den Berg, 2023). For example, in the marine bacterium *Alteromonas macleodii*, TBDR genes were selectively expressed in carbon- and iron-limiting conditions (Manck *et al.*, 2020) and during

polysaccharide utilization (Neumann *et al.*, 2015). Recently, it was shown that two of *T. turnerae's* four *TonB* genes are essential for growth in iron-limiting conditions and for growth with cellulose as a sole carbon source. This dependence indicates that the *TonB* system is essential for both iron acquisition and cellulose catabolism by *T. turnerae* (Naka and Haygood, 2023).

Interestingly, in a proteomic examination of the shipworm *Banka setacea*, a TBDR was the only major symbiont-derived protein observed in the cecum content that was not associated with the decomposition of lignocellulose (O'Connor *et al.*, 2014). This finding suggests the presence of symbiont outer membranes in the cecum. However, the cecum of shipworms has been shown by microscopic (Betcher *et al.*, 2012; Pesante *et al.*, 2021), transcriptomic (Sabbadin et al., 2018), and proteomic (O'Connor *et al.*, 2014) methods to be nearly devoid of intact bacterial cells. These observations argue against the transport of whole bacterial cells from the gill to the cecum as suggested in (Pesante *et al.*, 2021), but might suggest a role for OMVs in transporting lignocellulose degrading enzymes from the gill to the gut in shipworms.

Outer membrane vesicles are critical in bacterial interactions with many animal and plant hosts (Berleman and Auer, 2013; Lynch and Alegado, 2017). While most research has focused on pathogenic interactions, OMVs may also contribute to beneficial host-symbiont associations. For example, OMVs have been shown to mimic whole cells of *Vibrio fisheri* in the induction of specific aspects of light organ development in the Hawaiian bobtail squid *Euprymna scolopes* (Aschtgen *et al.*, 2016). OMVs have also been shown to be produced by chemoautotrophic symbionts that occur in the trophosome of flatworms of the genus

Paracatenula, where they play a critical role in provisioning the host with carbohydrates synthesized by the symbionts (Jäckle *et al.*, 2019). In the human gut microbiome, members of *Bacteroides* have been shown to tailor OMV content to specific polysaccharides (Sartorio *et al.*, 2023), and OMVs produced by human and ruminant gut bacteria, including Bacteroides, Fibrobacter, and Clostridium, communally degrade polysaccharides into nutrients available to the hosts (Rakoff-Nahoum *et al.*, 2014; Arntzen *et al.*, 2017; Gharechahi *et al.*, 2023).

Outer membrane vesicles can also transport proteins across the plasma membranes of eukaryotic organisms (O'Donoghue and Krachler, 2016; Schorey *et al.*, 2021; Toyofuku *et al.*, 2023). While previous research has focused mainly on the role of OMVs in introducing bacterial molecules into eukaryotic cells, OMVs may also transport molecules produced by intracellular bacteria out of their eukaryotic host. For example, *Salmonella enterica,* which grows in vesicles within their host's cells, produces toxin-loaded OMVs that escape the infected host cells and deliver their toxic cargo to uninfected neighboring cells (O'Donoghue and Krachler, 2016). Similarly, OMVs produced by *Mycobacterium tuberculosis* are released from infected macrophages, exporting Mycobacterial lipoproteins and lipoglycans that affect the immune functions of neighboring uninfected host cells (Athman *et al.*, 2015). Thus, OMV-mediated mechanisms could potentially explain the transport of cellulolytic proteins produced by *T. turnerae* in their intracellular location within the host's bacteriocytes to an extracellular location, allowing subsequent transport to the host's gut.

Packaging enzymes within OMVs or bound to OMV surfaces can have distinct advantages over their secretion as soluble proteins or proteins bound to the cell surface. For example, OMVs may protect proteins from degradation in the environment (Bonnington and Kuehn,

2014; Alves *et al.*, 2016; Zingl *et al.*, 2021), selectively concentrate proteins with specific functions (Orench-Rivera and Kuehn, 2021; Sartorio *et al.*, 2023), and deliver proteins to remote locations in sufficient quantity to produce a desired effect without the dilution that would be experienced by soluble proteins (Toyofuku *et al.*, 2023). These factors may be especially important for the degradation of complex substrates like lignocellulose, where the simultaneous delivery of specific sets of proteins in the correct proportions and spatial orientation can yield significant synergistic interactions that enhance efficiency (Park *et al.*, 2014).

However, little is known about OMV production and its function in environmental lignocellulose degradation. Several investigations of lignocellulose-degrading microorganisms from soil suggest OMVs play critical roles in terrestrial plant biomass degradation. For example, when grown in the presence of lignin, *Pseudomonas putida* produces OMVs containing enzymes functionally active against lignin aromatic components (Salvachúa *et al.*, 2020). Similarly, *Trichoderma reesei*, a filamentous fungus, produces OMVs containing a variety of cellulases when grown in the presence of cellulose (De Paula *et al.*, 2019).

In addition to their potential roles in shipworm symbiosis and the environmental turnover of lignocellulose in terrestrial and aquatic environments, cellulolytic OMVs are of significant interest in converting plant biomass into renewable liquid fuels or fine chemicals (Thakur *et al.*, 2023). A significant challenge in biomass conversion is understanding how cooperation among cellulases and associated enzymes can improve the design of efficient enzyme cocktails tailored to individual feedstocks (Østby *et al.*, 2020). OMVs produced by *T. turnerae* and other lignocellulolytic organisms may represent nature-based solutions that reveal specific combinations, concentrations, and spatial organization of cooperating enzymes that

433 significantly enhance lignocellulose degradation in nature and so might inspire the design of
434 engineered lignocellulose deconstruction systems.
435

436 ## Figure legends

437 Figure 1. Methods used to isolate and characterize outer membrane vesicles from *T. turnerae*.
438 Diagram showing: (A) bacterial culture, (B) OMV isolation based on differential and
439 density gradient separation, (C) OMV visualization and size by TEM and NTA, proteome
440 analysis by LC-MS/MS, and (D) detection of cellulase activity in purified OMV
441 preparations by zymography and reducing sugar (DNS) assay. Created with
442 BioRender.com.

443 Figure 2. Size, concentration, and visualization of OMVs isolated from *T. turnerae* culture
444 supernatants after growth on carboxymethyl cellulose (CMC). (A-B) Size distribution
445 and particle concentration for strains T7901 and SR01903, respectively. OMVs from
446 SR01903 were slightly larger in average size than OMVs from T7901. (C-D) Isolated
447 OMVs from strains T7901 and SR01903 were imaged using transmission electron
448 microscopy. Scale bar = 100 nm.

449 Figure 3. T. turnerae OMV proteome profiles. (A) Relative protein abundance grouped by
450 predicted subcellular location and (B) Clusters of Orthologous Groups (COG) functional
451 categories of identified proteins. (C) Top 10 STRINGdb pathways (ranked by FDR) found
452 in OMVs of T7901. Similar top pathways were found in OMVs of SR01903.

453 Figure 4. Carbohydrate-active modules and observed cellulase activity of *T. turnerae* OMVs. (A)
454 Heatmap profile of the relative abundance of the predicted carbohydrate-active
455 enzymes found in OMVs. (B) Denaturing SDS-PAGE (left) and zymogram (right; CMC

substrate) of isolated OMVs. (C) Histogram showing cellulase activity (CMC substrate) in Units/mg (as determined by DNS assay) for isolated OMVs and a purified cellulase enzyme cocktail (Cellulase R-10, Goldbio CAS# 9012-54-8). Bars indicate means (error bars: standard deviations of three replicates).

Author Contribution Statement

Mark T. Gasser: Conceptualization; investigation; formal analysis; methodology; writing – original draft preparation. **Annie Liu:** Investigation; methodology. **Marvin A. Altamia:** Investigation; methodology. **Bryan R. Brensinger:** Investigation; methodology. **Sarah L. Brewer:** Investigation; methodology. **Ron Flatau:** Investigation; methodology. **Eric R. Hancock:** Investigation; methodology. **Sarah P. Preheim:** Supervision; writing – review and editing. **Claire Marie Filone:** Funding acquisition; supervision; writing – review and editing. **Dan L. Distel:** Funding acquisition; Conceptualization; supervision; writing – original draft preparation; writing – review and editing.

Acknowledgments

We would like to thank the PennVet Extracellular Vesicle Core SCR_022444 (Philadelphia, Pennsylvania) for work and assistance with OMV isolation and NTA analysis; the University of Maryland School of Medicine's and School of Dentistry's Electron Microscopy Core Imaging Facility - EMCIF (Baltimore, Maryland) for work and assistance with TEM imaging; and the NYU Langone's Proteomics Laboratory SCR_017926 (New York, New York) for work and assistance with mass spectrometry analysis.

Supplemental Information

Figure_S1_SuppInfo.docx

Dataset_S1_SuppInfo.xlsx

References

Altamia, M.A. and Distel, D.L. (2022) Transport of symbiont-encoded cellulases from the gill to the gut of shipworms via the enigmatic ducts of Deshayes: a 174-year mystery solved. *Proc R Soc B* **289**: 20221478.

Altamia, M.A., Lin, Z., Trindade-Silva, A.E., Uy, I.D., Shipway, J.R., Wilke, D.V., et al. (2020) Secondary Metabolism in the Gill Microbiota of Shipworms (Teredinidae) as Revealed by Comparison of Metagenomes and Nearly Complete Symbiont Genomes. *mSystems* **5**: e00261-20.

Altamia, M.A., Shipway, J.R., Stein, D., Betcher, M.A., Fung, J.M., Jospin, G., et al. (2021) Teredinibacter haidensis sp. nov., Teredinibacter purpureus sp. nov. and Teredinibacter franksiae sp. nov., marine, cellulolytic endosymbiotic bacteria isolated from the gills of the wood-boring mollusc Bankia setacea (Bivalvia: Teredinidae) and emended description of the genus Teredinibacter. *International Journal of Systematic and Evolutionary Microbiology* **71**:.

Altamia, M.A., Shipway, J.R., Stein, D., Betcher, M.A., Fung, J.M., Jospin, G., et al. (2020) Teredinibacter waterburyi sp. nov., a marine, cellulolytic endosymbiotic bacterium isolated from the gills of the wood-boring mollusc Bankia setacea (Bivalvia: Teredinidae) and emended description of the genus Teredinibacter. *International Journal of Systematic and Evolutionary Microbiology* **70**: 2388–2394.

Altamia, M.A., Wood, N., Fung, J.M., Dedrick, S., Linton, E.W., Concepcion, G.P., et al. (2014) Genetic differentiation among isolates of *Teredinibacter turnerae,* a widely occurring intracellular endosymbiont of shipworms. *Molecular Ecology* **23**: 1418–1432.

Alves, N.J., Turner, K.B., Medintz, I.L., and Walper, S.A. (2016) Protecting enzymatic function through directed packaging into bacterial outer membrane vesicles. *Sci Rep* **6**: 24866.

Arntzen, M.Ø., Várnai, A., Mackie, R.I., Eijsink, V.G.H., and Pope, P.B. (2017) Outer membrane vesicles from *Fibrobacter succinogenes* S85 contain an array of carbohydrate-active enzymes with versatile polysaccharide-degrading capacity. *Environmental Microbiology* **19**: 2701–2714.

Aschtgen, M.-S., Wetzel, K., Goldman, W., McFall-Ngai, M., and Ruby, E. (2016) *Vibrio fischeri* -derived outer membrane vesicles trigger host development: OMV deliver signals in the squid/vibrio symbiosis. *Cellular Microbiology* **18**: 488–499.

Athman, J.J., Wang, Y., McDonald, D.J., Boom, W.H., Harding, C.V., and Wearsch, P.A. (2015) Bacterial Membrane Vesicles Mediate the Release of *Mycobacterium tuberculosis* Lipoglycans and Lipoproteins from Infected Macrophages. *The Journal of Immunology* **195**: 1044–1053.

518 Berleman, J. and Auer, M. (2013) The role of bacterial outer membrane vesicles for intra- and
519 interspecies delivery. *Environmental Microbiology* **15**: 347–354.
520 Betcher, M.A., Fung, J.M., Han, A.W., O'Connor, R., Seronay, R., Concepcion, G.P., et al. (2012)
521 Microbial Distribution and Abundance in the Digestive System of Five Shipworm Species
522 (Bivalvia: Teredinidae). *PLoS ONE* **7**: e45309.
523 Biller, S.J., Coe, A., Arellano, A.A., Dooley, K., Gong, J.S., Yeager, E.A., et al. (2022) Environmental
524 and taxonomic drivers of bacterial extracellular vesicle production in marine ecosystems,
525 Microbiology.
526 Biller, S.J., Schubotz, F., Roggensack, S.E., Thompson, A.W., Summons, R.E., and Chisholm, S.W.
527 (2014) Bacterial Vesicles in Marine Ecosystems. *Science* **343**: 183–186.
528 Blanvillain, S., Meyer, D., Boulanger, A., Lautier, M., Guynet, C., Denancé, N., et al. (2007) Plant
529 Carbohydrate Scavenging through TonB-Dependent Receptors: A Feature Shared by
530 Phytopathogenic and Aquatic Bacteria. *PLoS ONE* **2**: e224.
531 Bonnington, K.E. and Kuehn, M.J. (2014) Protein selection and export via outer membrane
532 vesicles. *Biochimica et Biophysica Acta (BBA) - Molecular Cell Research* **1843**: 1612–
533 1619.
534 Cai, Y.J., Chapman, S.J., Buswell, J.A., and Chang, S. (1999) Production and Distribution of
535 Endoglucanase, Cellobiohydrolase, and β-Glucosidase Components of the Cellulolytic
536 System of *Volvariella volvacea* , the Edible Straw Mushroom. *Appl Environ Microbiol* **65**:
537 553–559.
538 Caruana, J.C. and Walper, S.A. (2020) Bacterial Membrane Vesicles as Mediators of Microbe –
539 Microbe and Microbe – Host Community Interactions. *Front Microbiol* **11**: 432.
540 Cragg, S.M., Beckham, G.T., Bruce, N.C., Bugg, T.D., Distel, D.L., Dupree, P., et al. (2015)
541 Lignocellulose degradation mechanisms across the Tree of Life. *Current Opinion in*
542 *Chemical Biology* **29**: 108–119.
543 Cragg, S.M., Friess, D.A., Gillis, L.G., Trevathan-Tackett, S.M., Terrett, O.M., Watts, J.E.M., et al.
544 (2020) Vascular Plants Are Globally Significant Contributors to Marine Carbon Fluxes and
545 Sinks. *Annu Rev Mar Sci* **12**: 469–497.
546 Dahmen, N., Lewandowski, I., Zibek, S., and Weidtmann, A. (2019) Integrated lignocellulosic
547 value chains in a growing bioeconomy: Status quo and perspectives. *GCB Bioenergy* **11**:
548 107–117.
549 De Paula, R.G., Antoniêto, A.C.C., Nogueira, K.M.V., Ribeiro, L.F.C., Rocha, M.C., Malavazi, I., et al.
550 (2019) Extracellular vesicles carry cellulases in the industrial fungus Trichoderma reesei.
551 *Biotechnol Biofuels* **12**: 146.
552 Dhurve, G., Madikonda, A.K., Jagannadham, M.V., and Siddavattam, D. (2022) Outer Membrane
553 Vesicles of *Acinetobacter baumannii* DS002 Are Selectively Enriched with TonB-
554 Dependent Transporters and Play a Key Role in Iron Acquisition. *Microbiol Spectr* **10**:
555 e00293-22.
556 Distel, D.L., DeLong, E.F., and Waterbury, J.B. (1991) Phylogenetic characterization and in situ
557 localization of the bacterial symbiont of shipworms (Teredinidae: Bivalvia) by using 16S
558 rRNA sequence analysis and oligodeoxynucleotide probe hybridization. *Appl Environ*
559 *Microbiol* **57**: 2376–2382.
560 Distel, D.L., Morrill, W., MacLaren-Toussaint, N., Franks, D., and Waterbury, J. (2002)
561 Teredinibacter turnerae gen. nov., sp. nov., a dinitrogen-fixing, cellulolytic,

562 endosymbiotic gamma-proteobacterium isolated from the gills of wood-boring molluscs
563 (Bivalvia: Teredinidae). *International Journal of Systematic and Evolutionary*
564 *Microbiology* **52**: 2261–2269.
565 Fadeev, E., Carpaneto Bastos, C., Hennenfeind, J.H., Biller, S.J., Sher, D., Wietz, M., and Herndl,
566 G.J. (2023) Characterization of membrane vesicles in *Alteromonas macleodii* indicates
567 potential roles in their copiotrophic lifestyle. *microLife* **4**: uqac025.
568 Fischer, T., Schorb, M., Reintjes, G., Kolovou, A., Santarella-Mellwig, R., Markert, S., et al. (2019)
569 Biopearling of Interconnected Outer Membrane Vesicle Chains by a Marine
570 Flavobacterium. *Appl Environ Microbiol* **85**: e00829-19.
571 Frias, A., Manresa, A., De Oliveira, E., López-Iglesias, C., and Mercade, E. (2010) Membrane
572 Vesicles: A Common Feature in the Extracellular Matter of Cold-Adapted Antarctic
573 Bacteria. *Microb Ecol* **59**: 476–486.
574 Galperin, M.Y., Wolf, Y.I., Makarova, K.S., Vera Alvarez, R., Landsman, D., and Koonin, E.V. (2021)
575 COG database update: focus on microbial diversity, model organisms, and widespread
576 pathogens. *Nucleic Acids Research* **49**: D274–D281.
577 Ge, S.X., Jung, D., and Yao, R. (2020) ShinyGO: a graphical gene-set enrichment tool for animals
578 and plants. *Bioinformatics* **36**: 2628–2629.
579 Gharechahi, J., Vahidi, M.F., Sharifi, G., Ariaeenejad, S., Ding, X.-Z., Han, J.-L., and Salekdeh, G.H.
580 (2023) Lignocellulose degradation by rumen bacterial communities: New insights from
581 metagenome analyses. *Environmental Research* **229**: 115925.
582 Ghose, T.K. (1987) Measurement of cellulase activities. *Pure and Applied Chemistry* **59**: 257–
583 268.
584 Hervé, C., Rogowski, A., Blake, A.W., Marcus, S.E., Gilbert, H.J., and Knox, J.P. (2010)
585 Carbohydrate-binding modules promote the enzymatic deconstruction of intact plant
586 cell walls by targeting and proximity effects. *Proc Natl Acad Sci USA* **107**: 15293–15298.
587 Huang, Y., Nieh, M., Chen, W., and Lei, Y. (2022) Outer membrane vesicles (OMVs) enabled bio-
588 applications: A critical review. *Biotechnol Bioeng* **119**: 34–47.
589 Ichikawa, S., Ogawa, S., Nishida, A., Kobayashi, Y., Kurosawa, T., and Karita, S. (2019)
590 Cellulosomes localise on the surface of membrane vesicles from the cellulolytic
591 bacterium *Clostridium thermocellum*. *FEMS Microbiology Letters* **366**: fnz145.
592 Jäckle, O., Seah, B.K.B., Tietjen, M., Leisch, N., Liebeke, M., Kleiner, M., et al. (2019)
593 Chemosynthetic symbiont with a drastically reduced genome serves as primary energy
594 storage in the marine flatworm *Paracatenula*. *Proc Natl Acad Sci USA* **116**: 8505–8514.
595 Lau, W.Y.V., Hoad, G.R., Jin, V., Winsor, G.L., Madyan, A., Gray, K.L., et al. (2021) PSORTdb 4.0:
596 expanded and redesigned bacterial and archaeal protein subcellular localization
597 database incorporating new secondary localizations. *Nucleic Acids Research* **49**: D803–
598 D808.
599 Lynch, J.B. and Alegado, R.A. (2017) Spheres of Hope, Packets of Doom: the Good and Bad of
600 Outer Membrane Vesicles in Interspecies and Ecological Dynamics. *J Bacteriol* **199**:.
601 Manck, L.E., Espinoza, J.L., Dupont, C.L., and Barbeau, K.A. (2020) Transcriptomic Study of
602 Substrate-Specific Transport Mechanisms for Iron and Carbon in the Marine Copiotroph
603 Alteromonas macleodii. *mSystems* **5**: e00070-20.

McGavin, M., Lam, J., and Forsberg, C.W. (1990) Regulation and distribution of Fibrobacter succinogenes subsp. succinogenes S85 endoglucanases. *Appl Environ Microbiol* **56**: 1235–1244.

Naka, H. and Haygood, M.G. (2023) The dual role of TonB genes in turnerbactin uptake and carbohydrate utilization in the shipworm symbiont *Teredinibacter turnerae*. *Appl Environ Microbiol* **89**: e00744-23.

Neumann, A.M., Balmonte, J.P., Berger, M., Giebel, H., Arnosti, C., Voget, S., et al. (2015) Different utilization of alginate and other algal polysaccharides by marine *A lteromonas macleodii* ecotypes. *Environmental Microbiology* **17**: 3857–3868.

O'Connor, R.M., Fung, J.M., Sharp, K.H., Benner, J.S., McClung, C., Cushing, S., et al. (2014) Gill bacteria enable a novel digestive strategy in a wood-feeding mollusk. *Proc Natl Acad Sci USA* **111**: E5096–E5104.

O'Donoghue, E.J. and Krachler, A.M. (2016) Mechanisms of outer membrane vesicle entry into host cells: MicroReview - OMV entry into host cells. *Cellular Microbiology* **18**: 1508–1517.

Orench-Rivera, N. and Kuehn, M.J. (2021) Differential Packaging Into Outer Membrane Vesicles Upon Oxidative Stress Reveals a General Mechanism for Cargo Selectivity. *Front Microbiol* **12**: 561863.

Østby, H., Hansen, L.D., Horn, S.J., Eijsink, V.G.H., and Várnai, A. (2020) Enzymatic processing of lignocellulosic biomass: principles, recent advances and perspectives. *Journal of Industrial Microbiology and Biotechnology* **47**: 623–657.

Park, M., Sun, Q., Liu, F., DeLisa, M.P., and Chen, W. (2014) Positional Assembly of Enzymes on Bacterial Outer Membrane Vesicles for Cascade Reactions. *PLoS ONE* **9**: e97103.

Pesante, G., Sabbadin, F., Elias, L., Steele-King, C., Shipway, J.R., Dowle, A.A., et al. (2021) Characterisation of the enzyme transport path between shipworms and their bacterial symbionts. *BMC Biol* **19**: 233.

Pollet, R.M., Martin, L.M., and Koropatkin, N.M. (2021) TonB-dependent transporters in the Bacteroidetes: Unique domain structures and potential functions. *Molecular Microbiology* **115**: 490–501.

Ragauskas, A.J., Beckham, G.T., Biddy, M.J., Chandra, R., Chen, F., Davis, M.F., et al. (2014) Lignin Valorization: Improving Lignin Processing in the Biorefinery. *Science* **344**: 1246843.

Rakoff-Nahoum, S., Coyne, M.J., and Comstock, L.E. (2014) An Ecological Network of Polysaccharide Utilization among Human Intestinal Symbionts. *Current Biology* **24**: 40–49.

Sabbadin, F., Pesante, G., Elias, L., Besser, K., Li, Y., Steele-King, C., et al. (2018) Uncovering the molecular mechanisms of lignocellulose digestion in shipworms. *Biotechnol Biofuels* **11**: 59.

Salvachúa, D., Werner, A.Z., Pardo, I., Michalska, M., Black, B.A., Donohoe, B.S., et al. (2020) Outer membrane vesicles catabolize lignin-derived aromatic compounds in *Pseudomonas putida* KT2440. *Proc Natl Acad Sci USA* **117**: 9302–9310.

Sartorio, M.G., Pardue, E.J., Scott, N.E., and Feldman, M.F. (2023) Human gut bacteria tailor extracellular vesicle cargo for the breakdown of diet- and host-derived glycans. *Proc Natl Acad Sci USA* **120**: e2306314120.

Schorey, J.S., Cheng, Y., and McManus, W.R. (2021) Bacteria- and host-derived extracellular vesicles – two sides of the same coin? *Journal of Cell Science* **134**: jcs256628.

Schwechheimer, C. and Kuehn, M.J. (2015) Outer-membrane vesicles from Gram-negative bacteria: biogenesis and functions. *Nat Rev Microbiol* **13**: 605–619.

Silale, A. and Van Den Berg, B. (2023) TonB-Dependent Transport Across the Bacterial Outer Membrane. *Annu Rev Microbiol* **77**: 67–88.

Szklarczyk, D., Gable, A.L., Lyon, D., Junge, A., Wyder, S., Huerta-Cepas, J., et al. (2019) STRING v11: protein–protein association networks with increased coverage, supporting functional discovery in genome-wide experimental datasets. *Nucleic Acids Research* **47**: D607–D613.

Teather, R.M. and Wood, P.J. (1982) Use of Congo red-polysaccharide interactions in enumeration and characterization of cellulolytic bacteria from the bovine rumen. *Appl Environ Microbiol* **43**: 777–780.

Thakur, M., Dean, S.N., Caruana, J.C., Walper, S.A., and Ellis, G.A. (2023) Bacterial Membrane Vesicles for In Vitro Catalysis. *Bioengineering* **10**: 1099.

Toyofuku, M., Schild, S., Kaparakis-Liaskos, M., and Eberl, L. (2023) Composition and functions of bacterial membrane vesicles. *Nat Rev Microbiol* **21**: 415–430.

Veith, P.D., Chen, Y.-Y., Chen, D., O'Brien-Simpson, N.M., Cecil, J.D., Holden, J.A., et al. (2015) Tannerella forsythia Outer Membrane Vesicles Are Enriched with Substrates of the Type IX Secretion System and TonB-Dependent Receptors. *J Proteome Res* **14**: 5355–5366.

Voight, J.R. (2015) Xylotrophic bivalves: aspects of their biology and the impacts of humans. *Journal of Molluscan Studies* **81**: 175–186.

Waterbury, J.B., Calloway, C.B., and Turner, R.D. (1983) A Cellulolytic Nitrogen-Fixing Bacterium Cultured from the Gland of Deshayes in Shipworms (Bivalvia: Teredinidae). *Science* **221**: 1401–1403.

Yan, S. and Wu, G. (2013) Secretory pathway of cellulase: a mini-review. *Biotechnol Biofuels* **6**: 177.

Yang, J.C., Madupu, R., Durkin, A.S., Ekborg, N.A., Pedamallu, C.S., Hostetler, J.B., et al. (2009) The Complete Genome of Teredinibacter turnerae T7901: An Intracellular Endosymbiont of Marine Wood-Boring Bivalves (Shipworms). *PLoS ONE* **4**: e6085.

Yu, C., Chen, Y., Lu, C., and Hwang, J. (2006) Prediction of protein subcellular localization. *Proteins* **64**: 643–651.

Zakharzhevskaya, N.B., Vanyushkina, A.A., Altukhov, I.A., Shavarda, A.L., Butenko, I.O., Rakitina, D.V., et al. (2017) Outer membrane vesicles secreted by pathogenic and nonpathogenic Bacteroides fragilis represent different metabolic activities. *Sci Rep* **7**: 5008.

Zingl, F.G., Thapa, H.B., Scharf, M., Kohl, P., Müller, A.M., and Schild, S. (2021) Outer Membrane Vesicles of Vibrio cholerae Protect and Deliver Active Cholera Toxin to Host Cells via Porin-Dependent Uptake. *mBio* **12**: e00534-21.

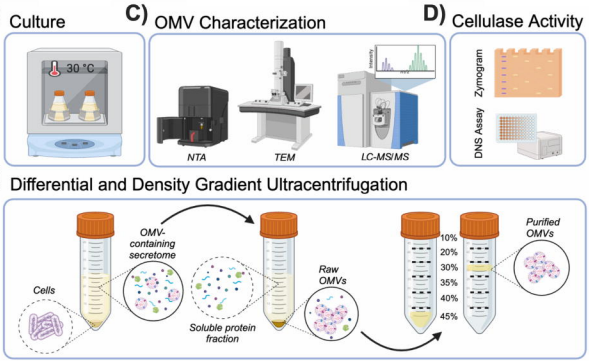
A)
Culture
30 °C
C)
OMV Characterization
NTA
TEM
LC-MS/MS
Intensity
D)
Cellulase Activity
Zymogram
DNS Assay
B)
Differential and Density Gradient Ultracentrifugation
Cells
OMV-containing secretome
Soluble protein fraction
Raw OMVs
10%
20%
30%
35%
40%
45%
Purified OMVs

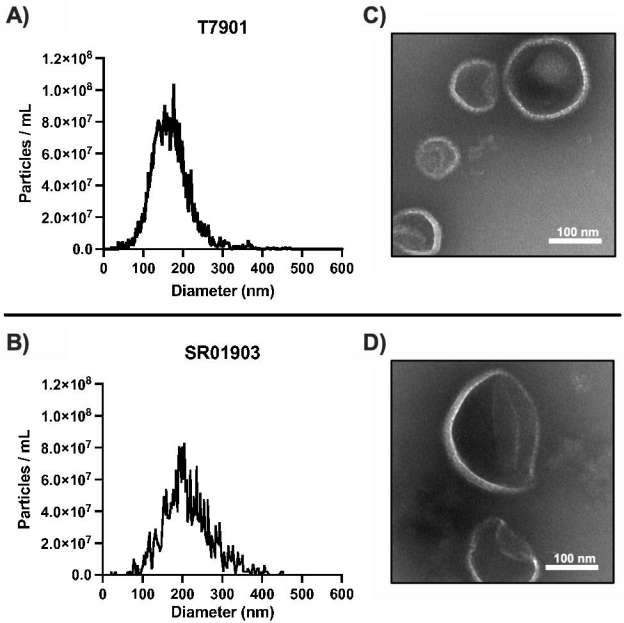
A)
T7901
Particles / mL
1.2×10^8
1.0×10^8
8.0×10^7
6.0×10^7
4.0×10^7
2.0×10^7
0.0
0
100
200
300
400
500
600
Diameter (nm)
C)
100 nm
B)
SR01903
Particles / mL
1.2×10^8
1.0×10^8
8.0×10^7
6.0×10^7
4.0×10^7
2.0×10^7
0.0
0
100
200
300
400
500
600
Diameter (nm)
D)
100 nm

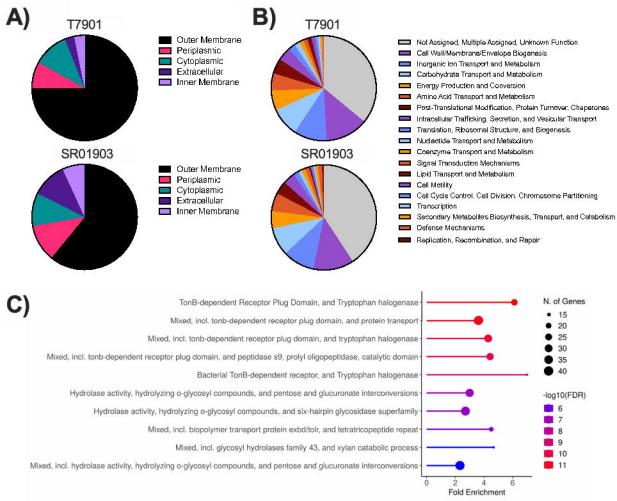
A)
T7901
Outer Membrane
Periplasmic
Cytoplasmic
Extracellular
Inner Membrane
SR01903
Outer Membrane
Periplasmic
Cytoplasmic
Extracellular
Inner Membrane
B)
T7901
SR01903
Not Assigned, Multiple Assigned, Unknown Function
Cell Wall/Membrane/Envelope Biogenesis
Inorganic Ion Transport and Metabolism
Carbohydrate Transport and Metabolism
Energy Production and Conversion
Amino Acid Transport and Metabolism
Post-Translational Modification, Protein Turnover, Chaperones
Intracellular Trafficking, Secretion, and Vesicular Transport
Translation, Ribosomal Structure, and Biogenesis
Nucleotide Transport and Metabolism
Coenzyme Transport and Metabolism
Signal Transduction Mechanisms
Lipid Transport and Metabolism
Cell Motility
Cell Cycle Control, Cell Division, Chromosome Partitioning
Transcription
Secondary Metabolites Biosynthesis, Transport, and Catabolism
Defense Mechanisms
Replication, Recombination, and Repair
C)
TonB-dependent Receptor Plug Domain, and Tryptophan halogenase
Mixed, incl. tonb-dependent receptor plug domain, and protein transport
Mixed, incl. tonb-dependent receptor plug domain, and tryptophan halogenase
Mixed, incl. tonb-dependent receptor plug domain, and peptidase s9, prolyl oligopeptidase, catalytic domain
Bacterial TonB-dependent receptor, and Tryptophan halogenase
Hydrolase activity, hydrolyzing o-glycosyl compounds, and pentose and glucuronate interconversions
Hydrolase activity, hydrolyzing o-glycosyl compounds, and six-hairpin glycosidase superfamily
Mixed, incl. biopolymer transport protein exbd/tolr, and tetratricopeptide repeat
Mixed, incl. glycosyl hydrolases family 43, and xylan catabolic process
Mixed, incl. hydrolase activity, hydrolyzing o-glycosyl compounds, and pentose and glucuronate interconversions
0
2
4
6
Fold Enrichment
N. of Genes
15
20
25
30
35
40
-log10(FDR)
6
7
8
9
10
11

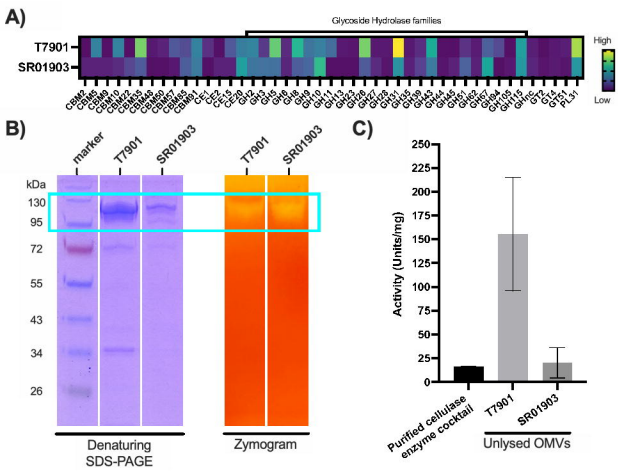
A)
Glycoside Hydrolase families
T7901
SR01903
High
Low
CBM4
CBM46
CBM49
CBM10
CBM35
CBM43
CBM59
CBM60
CBM62
CBM48
CBM61
CE1
CE7
CE12
GH2
GH3
GH5
GH8
GH9
GH10
GH11
GH13
GH26
GH27
GH28
GH31
GH36
GH39
GH42
GH43
GH44
GH45
GH67
GH94
GH101
GH115
GH10
GT2
GT4
GT51
PL1
B)
marker
T7901
SR01903
T7901
SR01903
kDa
130
95
72
55
43
34
26
Denaturing SDS-PAGE
Zymogram
C)
Activity (Units/mg)
250
225
200
175
150
125
100
75
50
25
0
Purified cellulase enzyme cocktail
T7901
SR01903
Unlysed OMVs